Article

The Isolation and Identification of Anthocyanin-Related GSTs in Chrysanthemum

Yajing Li [1,2,3,†], Xiaofen Liu [1,2,3,†], Fang Li [1,2], Lili Xiang [1,2,3,*] and Kunsong Chen [1,2,3]

1   College of Agriculture & Biotechnology, Zijingang Campus, Zhejiang University, Hangzhou 310058, China; liyajing_0526@163.com (Y.L.); lmqlxf119@163.com (X.L.); lifang68@zju.edu.cn (F.L.); akun@zju.edu.cn (K.C.)
2   Zhejiang Provincial Key Laboratory of Horticultural Plant Integrative Biology, Zijingang Campus, Zhejiang University, Hangzhou 310058, China
3   The State Agriculture Ministry Laboratory of Horticultural Plant Growth, Development and Quality Improvement, Zijingang Campus, Zhejiang University, Hangzhou 310058, China
*   Correspondence: 11516055@zju.edu.cn
†   These authors contributed equally to this work.

Abstract: Anthocyanin is the crucial pigment for the coloration of red chrysanthemum flowers, which synthesizes in the cytosol and is transported to the vacuole for stable storage. In general, glutathione S-transferases (GSTs) play a vital role in this transport. To date, there is no functional GST reported in chrysanthemums. Here, a total of 94 CmGSTs were isolated from the chrysanthemum genome, with phylogenetic analysis suggesting that 16 members of them were clustered into the Phi subgroup which was related to anthocyanin transport. Among them, the expression of *CmGST1* was positively correlated with anthocyanin accumulation. Protein sequence alignment revealed that CmGST1 included anthocyanin-related GST-specific amino acid residues. Further transient overexpression experiments in tobacco leaves showed that CmGST1 could promote anthocyanin accumulation. In addition, a dual-luciferase assay demonstrated that *CmGST1* could be regulated by *CmMYB6*, *CmbHLH2* and *CmMYB#7*, which was reported to be related to anthocyanin biosynthesis. Taken together, we suggested that CmGST1 played a key role in anthocyanin transport and accumulation in chrysanthemums.

Keywords: chrysanthemum; glutathione S-transferases; anthocyanins; transport

1. Introduction

The chrysanthemum (*Chrysanthemum morifolium* Ramat.) is one of the most popular ornamental plants in the world and flower color is a crucial trait for its commercial value [1]. Flower color is mainly contributed to by flavonoids, carotenoids and betalains [2]. Among them, anthocyanins, which belong to flavonoids, accumulate in red chrysanthemums.

Anthocyanins are one of the most important secondary metabolites and serve to protect plants from pathogen attacks and ultraviolet radiation damage [3,4]. Anthocyanins are synthesized in the cytosol and then transported into the vacuole for stable storage [5,6]. Biosynthetic genes in this process include chalcone synthase (*CHS*), chalcone isomerase (*CHI*), favanone 3-hydroxylase (*F3H*), flavonoid 3′-hydroxylase (*F3′H*), favonoid 3′, 5′-hydroxylase (*F3′5′H*), dihydrofavonol 4-reductase (*DFR*), anthocyanidin synthase (*ANS*), and UDP-glucose: favonoid-3-O-glucosyltransferase (*UFGT*). The studies on the structural genes of the synthesis pathway of anthocyanin are relatively clear, but there are still uncertainties about the transport mechanism of anthocyanin in chrysanthemums. Based on the previous results, there are two modes which have been proposed for anthocyanin transport: vesicle trafficking-mediated transport and membrane transporter-mediated transport [6]. In both modes glutathione S-transferases (GSTs) play a key role [6].

It is generally accepted that GSTs play an important role in the cellular redox control and detoxification of heavy metals, electrophilic xenobiotics, and the control of toxic

by-products in normal plant metabolism [7,8]. There are seven subgroups functionally characterized in the GST family, including Tau, Phi, zeta, theta, Dehydroascorbate reductase, TDL, and Lambda [9], where the anthocyanin-related GSTs belong to the Phi subgroup [10]. As for transport mechanisms, several studies suggested that GST promoted the accumulation of anthocyanins such as Bz2 in maize, by catalyzing the formation of the glutathione-conjugated complex [11]. However, more evidence showed that GSTs could not catalyze the formation of the glutathione-conjugated complex but promoted the vacuolar sequestration of anthocyanins, such as AN9 in petunias [12], TT19 in Arabidopsis [10], and VvGST1 and VvGST4 in grapvines [13]. Based on these findings, GSTs might act as a carrier to transport anthocyanin [6,14]. In recent years, many anthocyanin-related GSTs in different species have been identified. The gene *MdGSTF6* encoded an important GST transporter of anthocyanins in apple fruit [15]. The gene *PpGST1* played an important role in the color difference between 'Hujingmilu' and 'Yulu' [16]. The genes *LhGST* and *GhGSTF12* played an important role in the transport of anthocyanin in lily and cotton, respectively [17,18]. However, anthocyanin transport-related GSTs were rarely reported in ornamental horticulture. Therefore, an anthocyanin-related GST is reported in chrysanthemums in this study.

In this study, we screened 94 *GST*s from the chrysanthemum genome and identified *CmGST1* (*Cse sc027179.1 g030.1/pd*) in relation to anthocyanin in chrysanthemums, according to the transcript level in the flower developmental stages of the red chrysanthemum. It was localized in both the membrane and the nucleus. The gene CmGST1 promoted anthocyanin accumulation via the sequestration of glycosylated anthocyanin, based on the transient overexpression results in tobacco leaves. Furthermore, the transcript activity of the *CmGST1* promoter was regulated by anthocyanin-related transcription factors, including *CmMYB6*, *CmbHLH2* and *CmMYB#7*. Taken together, CmGST1 was responsible for anthocyanin transport in chrysanthemums and affected anthocyanin accumulation.

2. Materials and Methods

2.1. Plant Materials

The Chrysanthemum red series cultivar 'Monalisa pink' was obtained from Yunnan Fengdao Floriculture Company (Yunnan, China). The flowers were divided into 3 stages, which represented flower bud stage (stage 1, S1), half-bloom stage (stage 2, S2) and full-bloom stage (stage 3, S3), respectively. Among them, S2 and S3 included ray flowers and disc flowers. The ray flowers were named S2-R and S3-R and the disc flowers were named S2-D and S3-D, respectively. Three independent biological replicates were collected for each stage. The collected samples were immediately frozen in liquid nitrogen and then stored at −80 °C until used.

2.2. Extraction of RNA and DNA

Total RNA was extracted from chrysanthemum flowers using the CTAB method [19]. For tobacco leaves, total RNA was extracted using an RNAiso Plus (Takara, Japan) according to the manufacturer's instructions. Genomic DNA was isolated from chrysanthemum leaves by Easy Plant Genomic DNA Extraction Kit (Easy-Do, Hangzhou, China) according to the manufacturer's instructions.

2.3. cDNA Synthesis and qRT-PCR

First-strand cDNA was synthesized using PrimeScriptTM RT reagent Kit (Takara, Japan). RT-qPCR reactions were carried out with SsoFast EvaGreen Supermix kit (Bio-Rad, Hercules, CA, USA) using a CFX96 instrument (Bio-Rad, Hercules, CA, USA). The RT-qPCR program was initiated with the preliminary step of 3 min at 95 °C, followed by 45 cycles of 95 °C for 10 s, 60 °C for 30 s, 95 °C for 10 s, and then a continuous increase from 65 °C to 95 °C with a ramp rate of 0.5 °C/s for dissociation curve analysis. Data were analyzed and relative expression levels of the genes were calculated using the $2^{(-\triangle\triangle Ct)}$ method and using expression of the *CmActin* [1] as the internal control. The primers for

RT-qPCR analysis were listed in Table S1. Three biological replicates were performed in this experiment.

2.4. Phylogenetic Analysis of CmGSTs

CmGSTs were identified from Chrysanthemum genome (http://mum-garden.kazusa.or.jp Accessed on 6 August 2021). All amino acid sequences were used for constructing a phylogenetic tree, together with anthocyanin-related GSTs from other species. A phylogenetic tree was constructed by IqTree software with a bootstrap value of 1000 using maximum likelihood method.

2.5. Isolation and Sequence Analysis of CmGST1

CmGST1 sequences were isolated from cDNA of 'Monalisa Pink' flowers. The primers were designed according to RNA-seq (Table S2). According to a partial cDNA sequence, full-length cDNA sequence of *CmGST1* was amplified by RACE (rapid amplification of cDNA ends, Clontech, Mountain view, CA, USA).

The protein sequences were translated for sequence alignments by ExPASy (https://web.expasy.org/translate/ Accessed on 6 August 2021). The homologous comparison with anthocyanin-related GSTs was analyzed by DNAMAN 8. The anthocyanin-related GSTs from other species were from Genbank.

2.6. Vector Construction

Primers for vector construction were listed in Table S2. For overexpression, *CmMYB6-bHLH2* and *CmGST1* were cloned and inserted into pGreenII 0029 62-SK vector (CmMYB6-bHLH2-SK, CmGST1-SK). For subcellular location analysis, the *CmGST1* full-length coding sequence without the stop codon was fused to the pCAMBIA1300-eGFP vector (CmGST1-eGFP). Then, all of these constructs were electroporated into *Agrobacterium tumefaciens* strain EHA105 by the GenePulser XcellTM Electroporation Systems (Bio-Rad, Hercules, CA, USA). For dual-luciferase report assay, *CmMYB6*, *CmbHLH2* and *CmMYB#7* were cloned and inserted into pGreenII 0029 62-SK vector (CmMYB#7-SK), and the promoter of *CmGST1* (2000bp) was constructed into pGreen II 0800-LUC vector (CmGST1-LUC). Then, CmGST1-eGFP, CmMYB6-SK, CmbHLH2-SK, CmMYB#7-SK and CmGST1-LUC were electroporated into *Agrobacterium tumefaciens* strain GV3101 by the GenePulser XcellTM Electroporation Systems (Bio-Rad, Hercules, CA, USA).

2.7. Subcellular Location Analysis

The CmGST1-eGFP-GV3101 was fused to the membrane localization marker expressed transiently in transgenic *N. benthamiana* (with nucleus-located marker) leaves by infiltration. The cultures were adjusted OD600 to 0.75 with infiltration buffer (10 mM MES, 10 mM MgCl2, 150 mM acetosyringone, pH 5.6). The *N. benthamiana* leaves were observed using laser-scanning confocal microscope (Zeiss, lsm 880, Germany) 2 days after injecting.

2.8. Measurement of Anthocyanin

The anthocyanin contents of chrysanthemum flowers and tobacco leaves were detected by the pH differential spectrophotometry method described in our previous study [1]. Flower anthocyanin contents were extracted from 0.1 g samples of methanol/0.05% HCl at an absorbance of 510 and 700 nm. Three biological replicates were performed in this experiment.

2.9. Transient Overexpression on Tobacco Leaves

In order to verify the function of CmGST1 in inducing anthocyanin biosynthesis, transient overexpression in tobacco leaves (*Nicotiana tabacum*) was conducted as described in previous reports [20]. The *Agrobacterium* cultures with empty vectors, CmGST1 and CmMYB6-bHLH2, mixed with an empty vector or CmGST1, were infiltrated into tobacco

leaves, respectively. The patches in tobacco leaves were photographed 7 days after infiltration, then cut into pieces and frozen in liquid nitrogen before the detection of anthocyanin content. Each assay was carried out in three independent experiments with three biological replicates for each.

2.10. Gene Cloning and Analysis of the Promoter of CmGST1

Genomic DNA sequences were used for amplifying *CmGST1* promoter. The promoter region of *CmGST1* was amplified using primers designed by Chrysanthemum genome (http://mum-garden.kazusa.or.jp Accessed on 6 August 2021) (Table S2). *Cis*-elements were predicted using the PlantCARE program (https://bioinformatics.psb.ugent.be/webtools/plantcare/html/ Accessed on 6 August 2021).

2.11. Dual-Luciferase Report Assay

A dual-luciferase assay was widely used to analyze the transcriptional regulatory roles of transcription factors on target promoters [21–23]. All constructs were individually electroporated into *Agrobacterium tumefaciens* GV3101 (MP90) before being infiltrated into tobacco leaves (*Nicotiana benthamiana*). The enzyme activities of firefly luciferase (*CmGST1::LUC*) to renilla luciferase (*35S::REN*) were detected using a Dual-Luciferase Reporter Assay System (Promega, Wisconsin, MI, USA) and a Modulus Luminometer (Promega, Wisconsin, MI, USA). The ratio of LUC/REN was calculated to analyze the regulatory effect of the transcription factor on the promoter. Three independent experiments were carried out with at least four biological replicates for each.

3. Results

3.1. Identification and Phylogenetic Analysis of CmGSTs

A protein sequence of 94 CmGSTs were screened from the Chrysanthemum genome (http://mum-garden.kazusa.or.jp Accessed on 6 August 2021) based on annotations. A maximum likelihood tree was constructed using the Iqtree program, together with GSTs from Arabidopsis, and reported anthocyanin-related GSTs in other species. These GSTs were mainly divided into eight groups, where anthocyanin-related genes belonged to a Phi subgroup which included 16 CmGSTs (Figure 1). Sixteen GSTs were named in order according to their distance from ScGST3. The gene CmGST1 was clustered into the same branch as many other reported anthocyanin-related GSTs, such as ScGST3, CkmGST3, PhAN9, AcGST1, PpRiant1, FvRAP, and MdGST. Other GSTs were clustered into unknown GSTs from Arabidopsis. Thus, CmGST1 may have been a potential anthocyanin-related GST in chrysanthemums.

3.2. Anthocyanin Analysis in Different Developmental Stages of 'Monalisa Pink' Flower

'Monalisa Pink', which accumulated anthocyanin in the petals mainly contained three developmental stages during the flower development (Figure 2A). The three stages were named S1, S2 and S3, respectively, where the S2 and S3 were divided into ray flowers (S2-R, S3-R) and disc flowers (S2-D, S3-D). The total anthocyanin content in S1, S2-D, S3-D was undetected, but measured 0.024 mg/g and 0.309 mg/g in S2-R and S3-R, respectively (Figure 2B), consistent with the phenotype in Figure 2A.

3.3. Expression Patterns of CmGSTs of Phi Subgroup in Developmental Stages of 'Monalisa Pink' Flower Petals

A total of 16 *CmGST*s members were clustered into the Phi subgroup. However, their expression patterns showed significantly differences during the flower developmental stages, based on the results of RT-qPCR (Figure 2C). Among them, *CmGST1* and *CmGST13* exhibited higher expression levels in S2-R and S3-R, compared to S1, S2-D, and S3-D, which were consistent with a higher phenotype and anthocyanin content (Figure 2A,B), while the transcript levels of other *CmGST* members showed a weaker correlation with anthocyanin accumulation (Figure 2C). It is worth mentioning that the transcript levels of *CmGST1*
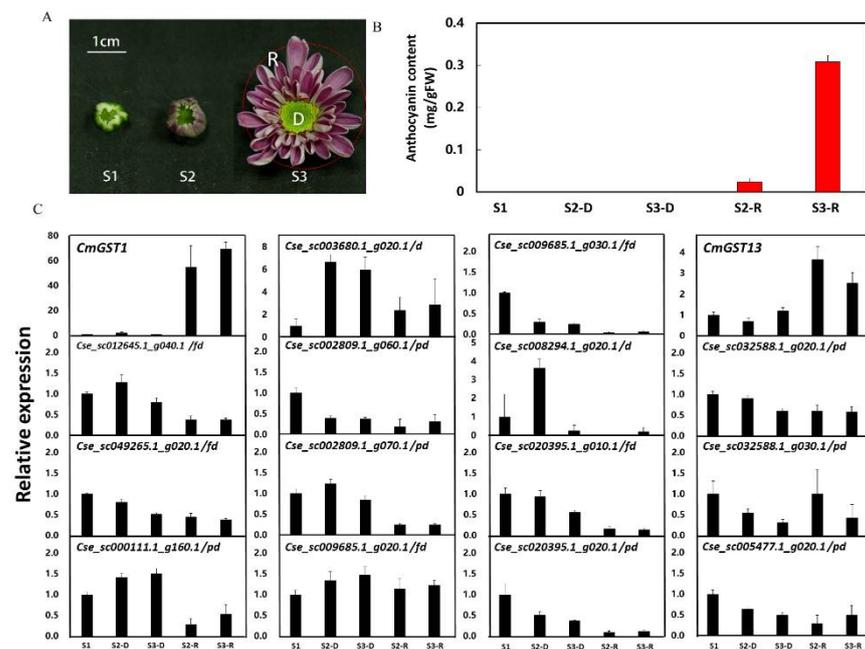
were 50 times higher than *CmGST13* (Figure 2C). Based on these results, there was stronger evidence for *CmGST1* being related to anthocyanin, rather that *CmGST13*.

3.4. Sequence Alignment of CmGST1 and CmGST13 in Chrysanthemum

Based on the previous results, most GSTs members clustered in the Phi subgroup contained GST-N-Phi (Thioredoxin-like superfamily) and GST-C-Phi (GST-C-family superfamily) domains, which included the glutathione binding sites (blue boxes, [24], Figure 3). Furthermore, the GSTs involved with anthocyanin transportation still contained anthocyanin-related GST-specific sites (red boxes) in these domains ([11], Figure 3).

Figure 1. Phylogenetic analysis of 94 CmGSTs with GSTs from Arabidopsis and reported anthocyanin-related GSTs in other species. The 94 CmGSTs proteins were obtained from the Chrysanthemum genome (http://mum-garden.kazusa.or.jp Accessed on 6 August 2021). The GenBank accession numbers were: PpRiant1 (ALE31199), MdGST (NP_001315851.1), FvRAP (XP_004288578), LcGST4 (ALY05893), VvGST4 (AAX81329), CMGSTF12 (ABA42223), ScGST3 (*Senecio cruentus*), AtTT19 (BAD89984), AcGST (QCQ77644), PhAN9 (CAA68993), CkmGST3 (BAM14584), The tree was constructed with the Maximum Likelihood method (1,000 replications of bootstrap test) using the Iqtree program.

Figure 2. Expression patterns of *CmGSTs* from Phi subclade in disc and ray flowers in developmental stage of 'Monalisa Pink'. (**A**) Phenotype of 'Monalisa Pink' at S1, S2-D, S3-D, S2-R, S3-R. (**B**) Anthocyanin contents of disc and ray flowers of different developmental stages. (**C**) Relative expression of disc and ray flowers. Data were means (±SE) from three independent biological replicates.
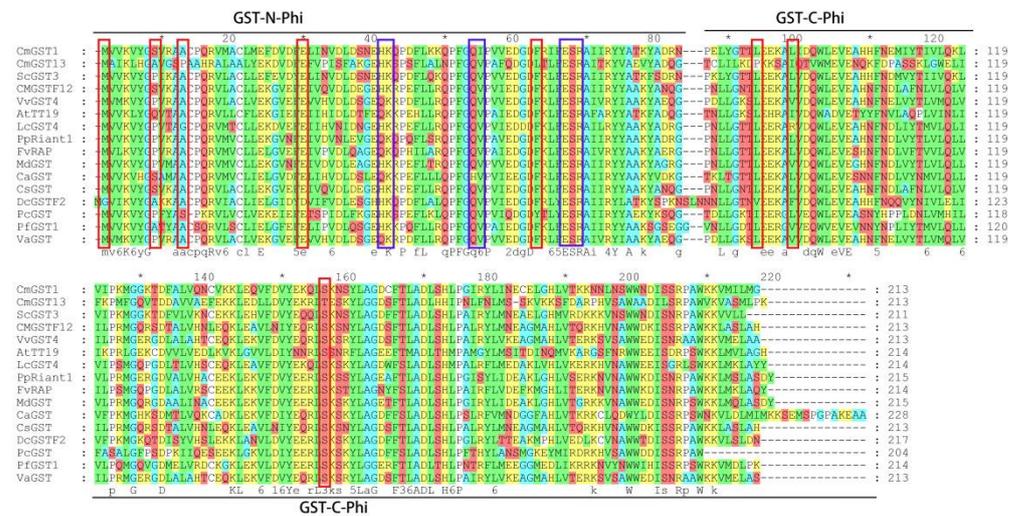

Figure 3. Multiple alignments of amino acid sequences for the CmGST1 and CmGST13 protein with other recognized anthocyanin-related GSTs. PpRiant1 (ALE31199), MdGST (NP_001315851.1), FvRAP (XP_004288578), LcGST4 (ALY05893), VvGST4 (AAX81329), VaGST (Vitis amurensis, ACN38271), CMGSTF12 (ABA42223), CsGST (Citrus sinensis, NP_001275781), CaGST (Capsicum annuum, XP_016562106), DcGSTF2 (Dianthus caryophyllus, BAM21533), ScGST3 (Senecio cruentus), AtTT19 (BAD89984), PfGST1 (Perilla frutescens, BAG14300), and PcGST (Pyrus communis, ABI79308). Red boxes indicated amino acid residues that had previously been recognized to be conserved in anthocyanin-related GST. Blue boxes indicated the regions that were involved in glutathione binding. Asterisks indicate a conserved amino acid site.

The multiple alignments of GSTs showed that CmGST1 included both glutathione binding sites and anthocyanin-related GST-specific sites, which were highly conserved with the known anthocyanin-related GST members, while CmGST13 only contained glutathione binding sites (Figure 3), which indicated CmGST1 was a potential function of GSTs related to anthocyanin transport.

3.5. Subcellular Localization of CmGST1

To analyze the subcellular localization of CmGST1, a transient expression system in *Nicotiana benthamiana* leaves labeled with a nuclear localization marker was used. A vacuolar membrane localization marker was injected into tobacco leaves together with *35S::CmGST1-GFP*, and the empty vector *35S::GFP* was set as a control. The leaves were observed under a laser-scanning confocal microscope 2 days after injection. It showed that *CmGST1-GFP* fluorescence was detected in both the vacuolar membrane and nucleus, combined with a marker (Figure 4) which suggested that CmGST1 was located in the vacuolar membrane and nucleus.
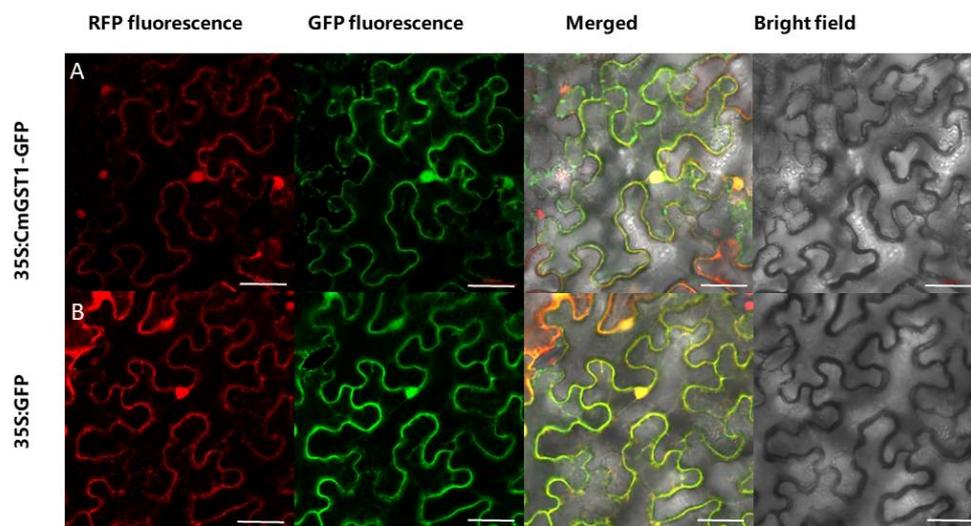

Figure 4. Subcellular localization analysis of CmGST1 in *Nicotiana benthamiana*. (**A**) Subcellular localization of *35S::CmGST1-GFP* together with the vacuolar membrane localization marker (RFP) and nuclear localization marker (RFP). (**B**) Subcellular localization of *35S::GFP* as control. Bars = 50 μm.

3.6. Transient Overexpression of CmGST1 in Tobacco Leaves

Transient overexpression was performed in tobacco leaves to examine the function of CmGST1 in vivo. Based on the previous studies, abundant anthocyanin could accumulate in tobacco leaves with the transient overexpression of *CmMYB6-bHLH2* which was an activator of anthocyanin transcript regulation [25]. Here, *35S::CmGST1* was injected into tobacco leaves together with *35S:: CmMYB6-bHLH2*, and the empty vector with *35S::CmMYB6-bHLH2* was set as a control. It suggested that the leaves' coloration, when co-injected with *35S::CmGST1* and *35S::CmMYB6-bHLH2*, were much darker than the control (Figure 5A), and the anthocyanin content of leaves was 0.3 mg/g and 0.15 mg/g, respectively (Figure 5B).

Moreover, the relative expressions of overexpressed genes and endogenous anthocyanin pathway genes, including biosynthetic and regulatory genes, were measured. The relative expressions of *CmMYB6* and *CmbHLH2* were almost at the same level between the empty vector and *CmGST1* combined with *CmMYB6-bHLH2* (Figure 5C). Nearly all structural genes' relative expressions increased in leaves infiltrated with *35S::CmGST1* and 35S::*CmMYB6-bHLH2*, compared to the control. When it comes to the transcription factors, only *NtAn1a* was upregulated after injecting *CmGST1* (Figure 6). This suggested

that CmGST1 promoted anthocyanin accumulation by sequestration of glycosylated anthocyanin, and then activated the anthocyanin pathway genes.
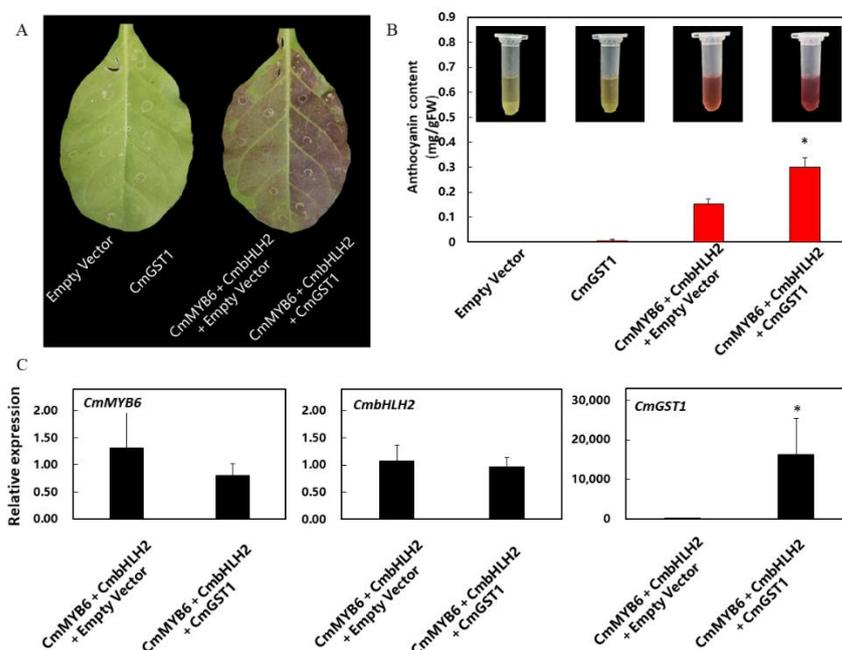

Figure 5. Transient overexpression of *35S::CmMYB6-bHLH2* together with *35S::CmGST1* in tobacco (*Nicotiana tabacum*) leaves. (**A**) A photograph of tobacco was taken at 7 days after injecting. (**B**) Anthocyanin content of tobacco leaves. (**C**) Transcriptional factors' relative expressions of transient overexpression of *35S::CmMYB6-bHLH2* and empty vector or *35S::CmGST1* in tobacco (*Nicotiana tabacum*) leaves. Data were means (±SE) from three independent biological replicates. Asterisks indicate significant differences (* P < 0.05).
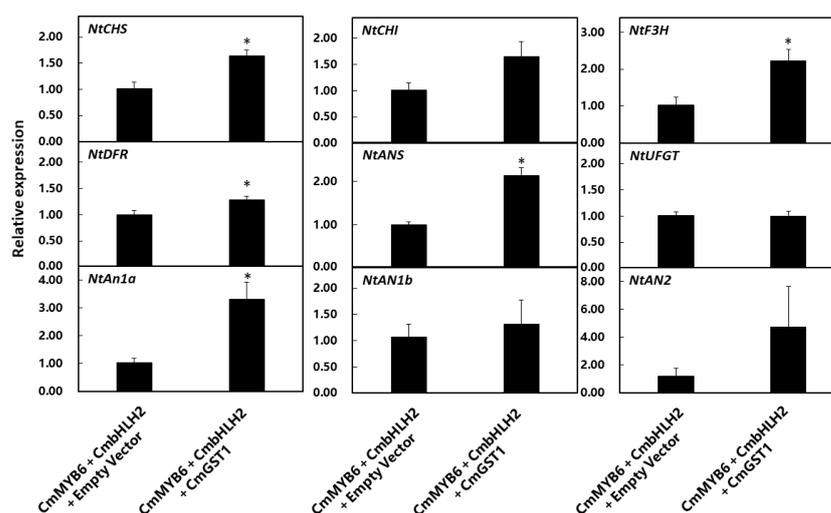

Figure 6. Structural genes and transcriptional factors' relative expressions of transient overexpression of *CmMYB6-bHLH2* and empty vector or *CmGST1* in tobacco (*Nicotiana tabacum*) leaves. Data were means (±SE) from three independent biological replicates. Asterisks indicate significant differences (* P < 0.05).

3.7. CmGST1 Promoter Was Regulated by Anthocyanin Related Transcription Factors

The promoter sequence of *CmGST1* which contained a 2,000 bp upstream region of ATG which was analyzed by the PlantCARE online tools (http://bioinformatics.psb.ugent.

be/webtools/plantcare/html/ Accessed on 6 August 2021). A total of seven MYB binding sites and 15 bHLH binding sites were found in the promoter (Figure 7A), as well as some *cis*-elements involved with MeJA, ABA, auxin, and light responsiveness (Table S3).
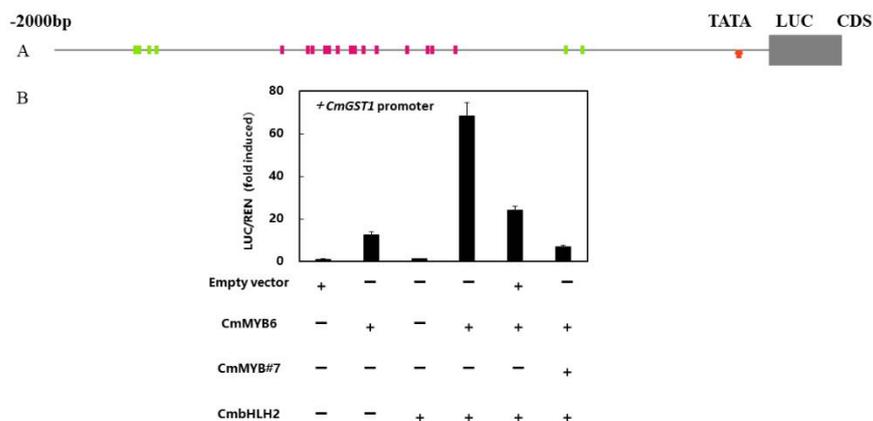

Figure 7. Regulatory effect of *CmMYB6*, *CmbHLH2* and *CmMYB#7* on the *CmGST1* promoter. (**A**) Schematics of *CmGST1* promoter, green rectangles meant that MYB recognized *cis*-elements and red rectangles meant that bHLH recognized *cis*-elements. TATA was labeled by a red arrow. (**B**) The regulatory effects of *CmMYB6*, *CmbHLH2* and *CmMYB#7* on the *CmGST1* promoter used dual-luciferase analysis. Data were means (±SE) from three independent biological replicates.

In the previous study, *CmMYB6*, *CmbHLH2*, and *CmMYB#7* were confirmed as playing essential roles in anthocyanin biosynthesis regulation. To study their relationship with *CmGST1*, dual-luciferase assays were performed. These assays suggested that *CmMYB6* increased the *CmGST1* promoter activity significantly by about 13 times compared to the control, while *CmbHLH2* had no effect (Figure 7B). Moreover, the much stronger trans-activation effect, which was approximately 70 higher times than the effect of the control on *CmGST1* promoter activity, was obtained by *CmMYB6* together with *CmbHLH2* (Figure 7B). In addition, *CmMYB#7* could reduce these activating effects on the *CmGST1* promoter by *CmMYB6* and *CmbHLH2* (Figure 7B).

4. Discussion

The enzymes encoded by anthocyanin-related structural genes and transport genes play a vital role in plants [26]. In transport-related gene families, the role of GSTs cannot be ignored [6]. The deletion or mutation of GSTs blocks anthocyanin transport and inhibits anthocyanin accumulation. The *Arabidopsis mutant tt19* cannot accumulate anthoyanin [10]. The gene PpRiant1 indicates that a small indel mutation in the Riant causes variegated colorations of peach flowers [27]. The gene FvRAP demonstrates that RAP encodes the principal GST transporters of anthocyanins and alters the fruit color in strawberries [28].

In general, the Phi subgroup contained a GST-N-Phi (Thioredoxin-like superfamily) domain and a GST-C-Phi (GST-C-family superfamily) domain [29]. Moreover, functional GSTs contained anthocyanin-related GST-specific sites [11]. In cotton leaves, a lack of partially anthocyanin-related GST-specific sites decreased anthocyanin accumulation [30]. In cyclamen, GSTs without anthocyanin-related sites could not recover anthocyanin accumulation in the *Arabidopsis tt19* mutant [11]. In these studies, most anthocyanin-related GSTs were identified by sequence similarity. Here, both CmGST1 and CmGST13 were clustered into the Phi subgroup with the conserved amino acid residues sites of the GST family and specific glutathione binding sites; however, only CmGST1 contained anthocyanin-related GST-specific sites. According to our analysis, CmGST13 was similar to other anthocyanin-nonrelated GSTs, especially at anthocyanin-related GST-specific sites [11]. Therefore, we predicted that CmGST13 could not promote anthocyanin accumulation.

Based on the previous results, there were mainly two modes of anthocyanin transport which included vesicle trafficking-mediated transport and membrane transporter-mediated transport [26,31]. Vesicle trafficking-mediated transport pathways were observed in many species, such as lisianthus, Arabidopsis, Brassica and sorghum, where glutathione S-transferases (GSTs) were proven to be relevant to this transport mode [31–33]. For membrane transporter-mediated transport, glutathione S-transferases (GSTs), ATP binding cassette (ABC) transporters and MATE transporters were a functional protein family involved in anthocyanin transport [26]. MATE transporters were mainly involved in transmembrane transport over short distances, and specifically transported acylated anthocyanin [21,34]. GSTs acted as an aid in the ABC-mediated transport mode for long-distance transport. Moreover, GSTs can function independently as a transporter [26]. This showed that GSTs played a widespread role in anthocyanin transport. In chrysanthemums, GSTs and MATEs were regarded as playing a vital role in flower color [35].

Several studies suggested GSTs were regulated by MYBs and bHLHs [15,16,36]. There were four MYB binding sites in peach (*PpGST1*), and five MYB binding sites in kiwifruit (*AcGST1*) [16,35]. In chrysanthemums, seven MYB binding sites were found in the promoter of *CmGST1* (Figure 7A). There were also 15 potential bHLH binding sites in the promoter of *CmGST1*, but *CmbHLH2* could not regulate *CmGST1* alone, which wasconsistent with other structural genes such as *CmDFR* and *CmUFGT* [37]. The gene *CmMYB6* could regulate *CmGST1*, either alone or mixed with *CmbHLH2*, and *CmMYB#7* could regulate *CmGST1* by competing with *CmMYB6*. These results showed that *CmMYB6* and *CmMYB#7* could regulate not only anthocyanin biosynthesis but also its transport process.

5. Conclusions

The gene CmGST1 was a key anthocyanin-related transporter in chrysanthemums, whose transcript was positively correlated with anthocyanin accumulation during flower development. The overexpression of CmGST1 in tobacco leaves promoted anthocyanin accumulation, and the expression of anthocyanin pathway genes was induced due to the sequestration of glycosylated anthocyanin. Furthermore, CmGST1 was regulated by previously characterized MYBs and bHLHs. Coloration is a crucial trait for ornamental horticulture, and our study provides a new target for flower breeding.

Author Contributions: Conceptualization, F.L. and K.C.; methodology, Y.L. and L.X.; software, Y.L.; validation, Y.L., L.X.; formal analysis, Y.L.; investigation, Y.L.; resources, F.L.; data curation, Y.L., L.X.; writing—original draft preparation, Y.L. and X.L.; writing—review and editing, X.L. and L.X.; visualization, Y.L.; supervision, K.C.; project administration, F.L., K.C. and L.X.; funding acquisition, F.L. and L.X. All authors have read and agreed to the published version of the manuscript.

Data Availability Statement: The datasets supporting the conclusions of this article are included.

Conflicts of Interest: The authors declare no conflict of interest.

References

1. Liu, X.F.; Xiang, L.L.; Yin, X.R.; Grierson, D.; Li, F.; Chen, K.S. The identification of a MYB transcription factor control ling anthocyanin biosynthesis regulation in Chrysanthemum flowers. *Sci. Hortic.* **2015**, *194*, 78–285. [CrossRef]
2. Tanaka, Y.; Sasaki, N.; Ohmiya, A. Biosynthesis of plant pigments: Anthocyanins, betalains and carotenoids. *Plant J.* **2008**, *54*, 733–749. [CrossRef] [PubMed]

3. Bieza, K.; Lois, R. An Arabidopsis mutant tolerant to lethal ultraviolet-B levels shows constitutively elevated accumulation of flavonoids and other phenolics. *Plant Physiol.* **2001**, *126*, 1105–1115. [CrossRef] [PubMed]
4. Veeriah, S.; Kautenburger, T.; Habermann, N.; Sauer, J.; Dietrich, H.; Will, F.; Pool-Zobel, B.L. Apple flavonoids inhibit growth of HT29 human colon cancer cells and modulate expression of genes involved in the biotransformation of xenobiotics. *Mol. Arcinogen.* **2006**, *5*, 164–174. [CrossRef]
5. Winkel-Shirley, B. Flavonoid biosynthesis. A colorful model for genetics, biochemistry, cell biology, and biotechnology. *Plant Physiol.* **2001**, *126*, 485–493. [CrossRef] [PubMed]
6. Zhao, J.; Dixon, R.A. The 'ins' and 'outs' of flavonoid transport. *Trends Plant Sci.* **2010**, *15*, 72–80. [CrossRef]
7. Brazier-Hicks, M.; Evans, K.M.; Cunningham, O.D.; Hodgson, D.R.W.; Steel, P.G.; Edwards, R. Catabolism of glutathi one conjugates in Arabidopsis thaliana. Role in metabolic reactivation of the herbicide safener fenclorim. *J. Biol. Chem.* **2008**, *283*, 21102–21112. [CrossRef] [PubMed]
8. Ketterer, B.; Meyer, D.J. Glutathione transferases: A possible role in the detoxication and repair of DNA and lipid hydroper oxides. *Mutat. Res.* **1989**, *214*, 33–40. [CrossRef]
9. Edwards, R.; Dixon, D.P. Plant glutathione transferases. *Gluthione Transferases Gamma-Glutamyl Transpeptidases* **2005**, *401*, 169–186.
10. Kitamura, S.; Shikazono, N.; Tanaka, A. TRANSPARENT TESTA 19 is involved in the accumulation of both anthocyanins and proanthocyanidins in Arabidopsis. *Plant J.* **2004**, *37*, 104–114. [CrossRef]
11. Kitamura, S.; Akita, Y.; Ishizaka, H.; Narumi, I.; Tanaka, A. Molecular characterization of an anthocyanin-related glutathi one S-transferase gene in cyclamen. *J. Plant Physiol.* **2012**, *169*, 636–642. [CrossRef] [PubMed]
12. Mueller, L.A.; Goodman, C.D.; Silady, R.A.; Walbot, V. AN9, a petunia glutathione S-transferase required for anthocyanin sequestration, is a flavonoid-binding protein. *Plant Physiol.* **2000**, *123*, 1561–1570. [CrossRef] [PubMed]
13. Conn, S.; Curtin, C.; Bezier, A.; Franco, C.; Zhang, W. Purification, molecular cloning, and characterization of glutathione S-transferases (GSTs) from pigmented Vitis vinifera L. cell suspension cultures as putative anthocyanin transport proteins. *J. Exp. Bot.* **2008**, *59*, 3621–3634. [CrossRef]
14. Sun, Y.; Li, H.; Huang, J.R. Arabidopsis TT19 functions as a carrier to transport anthocyanin from the cytosol to tonoplasts. *Mol. Plant.* **2012**, *5*, 387–400. [CrossRef]
15. Jiang, S.; Chen, M.; He, N.B.; Chen, X.L.; Wang, N.; Sun, Q.G.; Zhang, T.H.; Xu, H.F.; Fang, H.C.; Wang, Y.C.; et al. MdGSTF6, activated by MdMYB1, plays an essential role in anthocyanin accumulation in apple. *Hortic. Res.* **2019**, *6*, 1–14. [CrossRef]
16. Zhao, Y.; Dong, W.Q.; Zhu, Y.C.; Allan, A.C.; Wang, K.L.; Xu, C.J. PpGST1, an anthocyanin-related glutathione S-transfer ase gene, is essential for fruit coloration in peach. *Plant Biotechnol. J.* **2020**, *18*, 1284–1295. [CrossRef]
17. Cao, Y.W.; Xu, L.F.; Xu, H.; Yang, P.P.; He, G.R.; Tang, Y.C.; Song, M.; Ming, J. LhGST is an anthocyanin-related glutathi one S-transferase gene in Asiatic hybrid lilies (*Lilium* spp.). *Plant Cell Rep.* **2021**, *40*, 85–95. [CrossRef] [PubMed]
18. Shao, D.N.; Li, Y.J.; Zhu, Q.H.; Zhang, X.Y.; Liu, F.; Xue, F. GhGSTF12, a glutathione S-transferase gene, is essential for anthocyanin accumulation in cotton (*Gossypium hirsutum* L.). *Plant Sci.* **2021**, *305*, 110827. [CrossRef] [PubMed]
19. Chang, S.; Puryear, J.; Cairney, J. A simple and efficient method for isolating RNA from pine trees. *Mol. Biotechnol.* **2001**, *19*, 201–203. [CrossRef]
20. Liu, X.F.; Yin, X.R.; Allan, A.C.; Kui, L.W.; Shi, Y.N.; Huang, Y.J.; Ferguson, I.B.; Xu, C.J.; Chen, K.S. The role of MrbHLH1 and MrMYB1 in regulating anthocyanin biosynthetic genes in tobacco and Chinese bayberry (*Myrica rubra*) during anthocyanin biosynthesis. *Plant Cell Tissue Organ Cult.* **2013**, *115*, 285–298. [CrossRef]
21. Mathews, H.; Clendennen, S.K.; Caldwell, C.G.; Liu, X.L.; Connors, K.; Matheis, N.; Schuster, D.K.; Menasco, D.J.; Wagoner, W.; Lightner, J.; et al. Activation Tagging in Tomato Identifies a Transcriptional Regulator of Anthocyanin Biosynthesis, Modification, and Transport. *Plant Cell* **2003**, *15*, 1689–1703. [CrossRef]
22. Xu, Q.; Yin, X.R.; Zeng, J.K.; Ge, H.; Song, M.; Xu, C.J.; Li, X.; Ferguson, I.B.; Chen, K.S. Activator- and repressor-type MYB transcription factors are involved in chilling injury induced flesh lignification in loquat via their interactions with the phenylpropanoid pathway. *J. Exp. Bot.* **2014**, *65*, 4349–4359. [CrossRef] [PubMed]
23. Zeng, J.K.; Li, X.; Xu, Q.; Chen, J.Y.; Yin, X.R.; Ferguson, I.B.; Chen, K.S. EjAP2-1, an AP2/ERF gene, is a novel regulator of fruit lignification induced by chilling injury, via interaction with EjMYB transcription factors. *Plant Biotechnol. J.* **2015**, *13*, 1325–1334. [CrossRef] [PubMed]
24. Reinemer, P.; Prade, L.; Hof, P.; Neuefeind, T.; Huber, R.; Zettl, R.; Palme, K.; Schell, J.; Koelln, I.; Bartunik, H.D.; et al. Three-dimensional structure of glutathione S-transferase from Arabidopsis thaliana at 2.2 angstrom resolution: Structural characterization of herbicide-conjugating plant glutathione S-transferases and a novel active site architecture. *J. Mol. Biol.* **1996**, *255*, 289–309. [CrossRef] [PubMed]
25. Xiang, L.L.; Liu, X.F.; Li, X.; Yin, X.R.; Grierson, D.; Li, F.; Chen, K.S. A Novel bHLH Transcription Factor Involved in Regulating Anthocyanin Biosynthesis in Chrysanthemums (*Chrysanthemum morifolium* Ramat). *PLoS ONE* **2015**, *10*, e0143892. [CrossRef] [PubMed]
26. Zhao, J. Flavonoid transport mechanisms: How to go, and with whom. *Trends Plant Sci.* **2015**, *20*, 576–585. [CrossRef]
27. Cheng, J.; Liao, L.; Zhou, H.; Gu, C.; Wang, L.; Han, Y.P. A small indel mutation in an anthocyanin transporter causes var iegated colouration of peach flowers. *J. Exp. Bot.* **2015**, *66*, 7227–7239. [CrossRef]
28. Luo, H.F.; Dai, C.; Li, Y.P.; Feng, J.; Liu, Z.C.; Kang, C.Y. Reduced Anthocyanins in Petioles codes for a GST anthocyanin transporter that is essential for the foliage and fruit coloration in strawberry. *J. Exp. Bot.* **2018**, *69*, 2595–2608. [CrossRef]

29. Zhao, Y.; Dong, W.Q.; Wang, K.; Zhang, B.; Allan, A.C.; Lin, W.K.; Chen, K.S.; Xu, C.J. Differential Sensitivity of Fruit Pigmentation to Ultraviolet Light between Two Peach Cultivars. *Front. Plant Sci.* **2017**, *8*, 1552. [CrossRef]

30. Li, S.Y.; Zuo, D.Y.; Cheng, H.L.; Ali, M.; Wu, C.F.; Ashraf, J.; Zhang, Y.P.; Feng, X.X.; Lin, Z.X.; Wang, Q.L.; et al. Glutathione S-transferases GhGSTF1 and GhGSTF2 involved in the anthocyanin accumulation in *Gossypium hirsutum* L. *Int. J. Biol. Macromol.* **2020**, *165*, 2565–2575. [CrossRef] [PubMed]

31. Zhao, J.; Dixon, R.A. MATE Transporters Facilitate Vacuolar Uptake of Epicatechin 3′-O-Glucoside for Proanthocyanidin Biosynthesis in Medicago truncatula and Arabidopsis. *Plant Cell* **2010**, *22*, 991. [CrossRef] [PubMed]

32. Poustka, F.; Irani, N.; Feller, A.; Lu, Y.H.; Pourcel, L.; Frame, K.; Grotewold, E. A trafficking pathway for Anthocyanins overlaps with the endoplasmic reticulum-to-vacuole protein-sorting route in Arabidopsis and contributes to the formation of vacuolar inclusions. *Plant Physiol.* **2007**, *145*, 1323–1335. [CrossRef] [PubMed]

33. Zhang, H.B.; Wang, L.; Deroles, S.; Bennett, R.; Davies, K. New insight into the structures and formation of anthocyanic vacuolar inclusions in flower petals. *BMC Plant Biol.* **2006**, *6*, 1–4. [CrossRef]

34. Gomez, C.; Terrier, N.; Torregrosa, L.; Vialet, S.; Fournier-Level, A.; Verries, C.; Souquet, J.M.; Mazauric, J.P.; Klein, M.; Cheynier, V. Grapevine MATE-Type Proteins Act as Vacuolar H+-Dependent Acylated Anthocyanin Transporters. *Plant Physiol.* **2009**, *150*, 402–415. [CrossRef] [PubMed]

35. Kim, S.H.; Sung, S.Y.; Kim, Y.S.; Jo, Y.D.; Kang, S.Y.; Kim, J.B.; Ahn, J.W.; Ha, B.K.; Kim, D.S. Isolation and characteri zation of differentially expressed genes in petals of chrysanthemum mutant cultivars developed by irradiation. *Sci. Hortic.* **2015**, *189*, 132–138. [CrossRef]

36. Liu, Y.F.; Qi, Y.W.; Zhang, A.; Wu, H.X.; Liu, Z.D.; Ren, X.L. Molecular cloning and functional characterization of AcGST1, an anthocyanin-related glutathione S-transferase gene in kiwifruit (Actinidia chinensis). *Plant Mol. Biol.* **2019**, *100*, 451–465. [CrossRef]

37. Xiang, L.L.; Liu, X.F.; Li, H.; Yin, X.R.; Grierson, D.; Li, F.; Chen, K.S. CmMYB#7, an R3 MYB transcription factor, acts as a negative regulator of anthocyanin biosynthesis in chrysanthemum. *J. Exp. Bot.* **2019**, *70*, 3111–3123. [PubMed]